Inorg. Chem. **2006**, *45*, 1338−1348

O_2 and CO Binding to Tetraaza-Tripodal-Capped Iron(II) Porphyrins

Christian Ruzié,[†] Pascale Even,[†] David Ricard,[†] Thierry Roisnel,[‡] and Bernard Boitrel*[,†]

Université de Rennes 1, Institut de Chimie, UMR CNRS 6509, Organométalliques et Catalyse, Chimie et Electrochimie Moléculaire, 35042 Rennes Cedex, France and Université de Rennes 11, Institut de Chimie, UMR CNRS 6511, Laboratoire de Chimie du Solide et Inorganique Moléculaire, 35042 Rennes Cedex, France

Received August 27, 2005

A series of tris(2-aminoethylamine) (tren) capped iron(II) porphyrins has been synthesized and characterized and their affinities for dioxygen and carbon monoxide measured. The X-ray structure of the basic scaffold with nickel inserted in the porphyrin is also reported. All the ligands differ by the nature of the group(s) attached to the secondary amine functions of the cap. These various substitutions were introduced to probe if a hydrogen bond with these secondary amine groups acting as the donor could rationalize the high affinity of these myoglobin models. This work clearly indicates that the cage structure of the tren predominates over all the other appended groups with the exception of *p*-nitrophenol.

Introduction

Dioxygen transport, storage, and activation are the three critical steps of all aerobic life and performed by hemoproteins in vertebrates.[1] For the latter reaction the hemoprotein coordination site is a copper hemoprotein (cytochrome *c* oxidase) and the bound dioxygen is presumably interacting with copper(I) above the iron porphyrin in a light off-centered location.[2] In the case of dioxygen storage and transport (myoglobin (Mb)[3] and hemoglobin (Hb))[4] the coordination site is composed of a single heme buried in a hydrophobic pocket. In this instance the bound dioxygen does not interact with a second metal but with a histidine residue E7 positioned over the iron atom to be able to establish a hydrogen bond with the superoxo complex (Pauling hypothesis).[5] This hydrogen bond is considered to stabilize the dioxygen adduct. On the other hand, this same histidine residue could be also responsible for steric interactions with heme-bound carbon monoxide, which binds in an upright fashion. Indeed, the close proximity of His E7 to the ligand binding site led to the proposal that this residue could serve to hinder sterically the binding of CO and thus reduce its affinity for myoglobin and hemoglobin (Collman hypothesis).[6] This hypothesis of steric hindrance explains how nature has solved—partially at least—the problem of carbon monoxide toxicity without steric constraint on O_2 binding as the latter binds in a bent orientation.[7] Indeed, the natural affinity of the heme prosthetic group for CO is about 2×10^4 higher than that for O_2. This ratio is reduced around 200 for the proteins. Actually, the discrimination against CO allows the protein to decrease the CO affinity by a factor 100. Undoubtedly, the biomimetic studies initiated some 30 years ago have permitted a better comprehension of these observations. During this period of time iron complexes of various superstructured porphyrins have been elaborated in order to mimic the microenvironment of the prosthetic groups of dioxygen carrier hemoproteins.

The very first milestone is undeniably represented by the "picket-fence" porphyrin which is still the only model of

* To whom correspondence should be addressed. Phone: +33(2)2323 5856. Fax: +33(2)2323 5637. E-mail: Bernard.Boitrel@univ-rennes1.fr.
† UMR CNRS 6509.
‡ UMR CNRS 6511.

(1) (a) Zubay, G. *Biochemistry*; Addison-Wesley Publishing Co.: New York, 1983. (b) Stryer, L. In *Biochemistry*, 4th ed.; Freeman: 1995; pp 147−180.
(2) (a) Tsukihara, T.; Aoyama, H.; Yamashita, E.; Tomizaki, T.; Yamaguchi, H.; Shinzawa-Itoh, K.; Nakashima, R.; Yaono, R.; Yoshikawa, S. *Science* **1995**, *269*, 1069−1074. (b) Iwata, S.; Ostermeier, C.; Ludwig, B.; Michel, H. *Nature* **1995**, *376*, 660−669. (c) Yoshikawa, S.; Shinzawa-Itoh, K.; Nakashima, R.; Yaono, R.; Yamashita, E.; Inoue, N.; Yao, M.; Fei, M. J.; Libeu, C. P.; Mizushima, T.; Yamaguchi, H.; Tomizaki, T.; Tsukihara, T. *Science* **1998**, *280*, 1723−1729.
(3) Kendrew, J. C.; Dickerson, R. E.; Strandberg, B. E.; Hart, R. G.; Phillips, D. C.; Shore, V. C. *Nature* **1960**, *185*, 422−427.
(4) Perutz, M. F.; Rossmann, M. G.; Cullis, A. F.; Muirhead, H.; Will, G.; North, A. C. T. *Nature* **1960**, *185*, 416−422.
(5) Pauling, L. *Nature* **1964**, *203*, 182−183.
(6) Collman, J. P.; Brauman, J. I.; Halbert, T. R.; Suslick, K. S. *Proc. Natl. Acad. Sci. U.S.A.* **1976**, *73*, 3333−3337.
(7) (a) Li, X.-Y.; Spiro, T. G. *J. Am. Chem. Soc.* **1988**, *110*, 6024−6033. (b) Ray, G. B.; Li, X. Y.; Ibers, J. A.; Sessler, J. L.; Spiro, T. G. *J. Am. Chem. Soc.* **1994**, *116*, 162−176. (c) Spiro, T. G.; Kozlowski, P. M. *Acc. Chem. Res.* **2001**, *34*, 137−144.

10.1021/ic0514703 CCC: $33.50
Published on Web 01/06/2006

Table 1. Dioxygen and Carbon Monoxide Affinities of Models **1**, **3**−**9**, and Related Compounds from the Literature[a]

	solvent	$P_{1/2}(O_2)$ (Torr)	$P_{1/2}(CO)$ (Torr)	$M\,P_{1/2}(O_2)/P_{1/2}(CO)$
Mb[34]	H_2O, pH 7	0.37−1	$1.4-2.5 \times 10^{-2}$	20−40
Ascaris[17]	H_2O, pH 7	2×10^{-3}	0.1	0.02
Fe(picket fence)(1,2-Me_2Im)[11]	toluene, 25 °C	38	8.9×10^{-3}	4280
FeMedPoc(1-MeIm)[11]	toluene, 25 °C	0.36	6.5×10^{-4}	270
Fe-aBHP(C_3PyC_3)(C_{12})[12c,13 *b*]	toluene, 20 °C	2	9×10^{-5}	2×10^4
1 (2-MeIm)[19]	toluene, 25 °C	9.8×10^{-5}	3.1×10^{-4}	0.32
3 (2-MeIm)	toluene, 25 °C	2.4×10^{-5}	$<10^{-7}$	na
4 (1,2-Me_2Im)	toluene, 25 °C	2.7×10^{-4}	$<10^{-7}$	na
5 (2-MeIm)	toluene, 25 °C	0.18	nd	nd
5 (2-MeIm)	CH_2Cl_2, 25 °C	0.67	7×10^{-3}	96.4
6 (2-MeIm)[19]	toluene, 25 °C	4.0×10^{-6}	8.8×10^{-6}	0.46
7 (2-MeIm)	toluene, 25 °C	1.2×10^{-6}	1.7×10^{-6}	0.71
8 (2-MeIm)	toluene, 25 °C	10^{-6}	7×10^{-7}	1.43
9[b]	toluene, 25 °C	1.6×10^{-5}	$<10^{-7}$	na

[a] na: not accessible. nd: not determined. [b] Models bearing an internal fifth ligand.

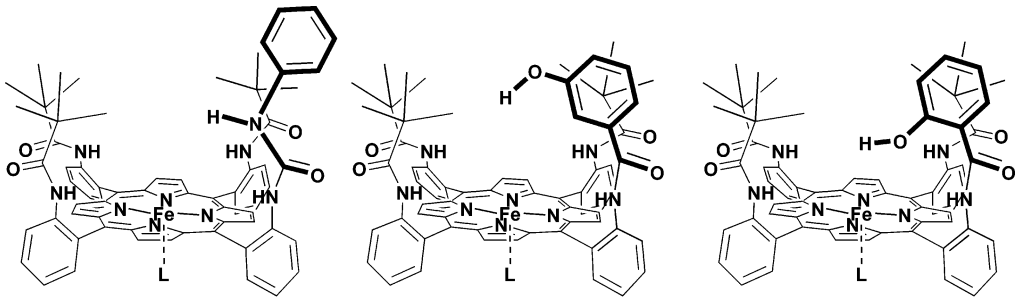

Figure 1. Chemical structure of three myoglobin models reported by Reed et al.[15] with the different X−H dipoles indicated: (a) phenylurea, (b) 3-phenol, and (c) 2-phenol; L = 1,2-Me_2Im.

oxy-myoglobin isolated in the solid state.[8] With this molecule it was demonstrated that similar affinities to those exhibited by the natural proteins could be reached and that the fence concept was efficient to prevent formation of the μ-oxodimer.[9] Since then so many other models have been proposed that only the reading of overviews can summarize the different approaches.[10] However, among them different specific ligands or families of ligands are worth being detailed. The family of "pocket porphyrins" provided supporting evidence for the steric influence on CO binding. Indeed, additional steric hindrance around the binding site resulted in unaltered dioxygen affinity but decreased carbon monoxide affinity.[11] In another study Momenteau et al. clearly demonstrated with two basket-handle porphyrins differing only by the linkage of the straps—either ether or amide—that the iron(II) complex bearing the straps via an amide linkage, one of them delivering a built-in nitrogen base, exhibited a dioxygen affinity 10 times greater than the ether-linked strapped porphyrin (Table 1, entry 5).[12] This 10-fold increase in O_2 affinity was attributed to a hydrogen bond between the terminal oxygen atom of the iron(II)-bound dioxygen and the NH of the meso-aromatic amide linkage.[13] In another report the size of the cavity from a "picnic-basket" porphyrin was systematically varied by changing the length of the linker between the two straps. It was shown that as the picnic-basket cavity becomes smaller, the H-bond or dipole−dipole interactions and the dioxygen affinity increase.[14] In 1995 systematic variation of one picket from the picket fence was described by Reed et al.[15] Interestingly, they reported a 10-fold increase of dioxygen affinity for the compound bearing either a phenyl urea-linked picket (Figure 1a) or a *m*-phenol amido-linked picket (Figure 1b). It has to be underlined that with these particular examples the location of the hydrogen-bond donor is changed and shifted toward

(8) (a) Collman, J. P.; Gagne, R. R.; Halbert, T. R.; Marchon, J.-C.; Reed, C. A. *J. Am. Chem. Soc.* **1973**, *95*, 7868−7870. (b) Collman, J. P.; Gagne, R. R.; Reed, C. A.; Halbert, T. R.; Lang, G.; Robinson, W. T. *J. Am. Chem. Soc.* **1975**, *97*, 1427−1439. (c) Jameson, G. B.; Rodley, G. A.; Robinson, W. T.; Gagne, R. R.; Reed, C. A.; Collman, J. P. *Inorg. Chem.* **1978**, *17*, 850−857. (d) Jameson, G. B.; Molinaro, F. S.; Ibers, J. A.; Collman, J. P.; Brauman, J. I.; Rose, E.; Suslick, K. S. *J. Am. Chem. Soc.* **1980**, *102*, 3224−3237.

(9) (a) Chin, D.-H.; DelGaudio, J.; LaMar, G. N.; Balch, A. L. *J. Am. Chem. Soc.* **1977**, *99*, 5486−5488. (b) Chin, D. H.; Mar, G. N. L.; Balch, A. L. *J. Am. Chem. Soc.* **1980**, *102*, 4344−4349.

(10) (a) Momenteau, M.; Reed, C. A. *Chem. Rev.* **1994**, *94*, 659−698. (b) Collman, J. P. *Inorg. Chem.* **1997**, *36*, 5145−5155. (c) Collman, J. P.; Fu, L. *Acc. Chem. Res.* **1999**, *32*, 455−463. (d) Collman, J. P.; Boulatov, R.; Sunderland, C. J.; Fu, L. *Chem. Rev.* **2004**, *104*, 561−588.

(11) (a) Collman, J. P.; Brauman, J. I.; Collins, T. J.; Iverson, B. L.; Lang, G.; Pettman, R. B.; Sessler, J. L.; Walter, M. A. *J. Am. Chem. Soc.* **1983**, *105*, 3038−3052. (b) Collman, J. P.; Brauman, J. I.; Iverson, B. L.; Sessler, J. L.; Morris, R. M.; Gibson, Q. H. *J. Am. Chem. Soc.* **1983**, *105*, 3052−3064.

(12) (a) Momenteau, M.; Mispelter, J.; Loock, B.; Bisagni, E. *J. Chem. Soc., Perkin Trans. 1* **1983**, 189−196. (b) Momenteau, M.; Mispelter, J.; Loock, B.; Lhoste, J.-M. *J. Chem. Soc., Perkin Trans. 1* **1985**, 61−70. (c) Momenteau, M.; Mispelter, J.; Loock, B.; Lhoste, J.-M. *J. Chem. Soc., Perkin Trans. 1* **1985**, 221−231. (d) Momenteau, M.; Loock, B.; Huel, C.; Lhoste, J.-M. *J. Chem. Soc., Perkin Trans. 1* **1988**, 283−295.

(13) Mispelter, J.; Momenteau, M.; Lavalette, D.; Lhoste, J.-M. *J. Am. Chem. Soc.* **1983**, *105*, 5165−5166.

(14) Collman, J. P.; Zhang, X. M.; Wong, K.; Brauman, J. I. *J. Am. Chem. Soc.* **1994**, *116*, 6245−6251.

(15) Wuenschell, G. E.; Tétreau, C.; Lavalette, D.; Reed, C. A. *J. Am. Chem. Soc.* **1992**, *114*, 3346−3355.

a more apical position. On the other hand, for the *o*-phenol amido-linked picket (Figure 1c) no effect was detected relative to the picket-fence reference compound. Almost 10 years later an unprecedented noncoordination of carbon monoxide at atmospheric pressure was reported with a cyclam-capped porphyrin, demonstrating the effect of steric interactions on porphyrin CO affinities.[16] It is worth noting that the latter was synthesized starting from a cyclic tetraamine with a resulting distance between the mean porphyrin plane and the N4-cyclam plane of 3.91 Å. Finally, a very high O_2 affinity, close to the Hb from *Ascaris*,[17] has been reported with dendritic porphyrins.[18] Some time later we reported a very high O_2 affinity as well,[19] obtained with the first generation of tren-capped iron(II) porphyrins lacking a built-in fifth ligand.[20] As this type of Mb model bears secondary amino functions in an apical position relative to the meso-aromatic amide linkage, we explained this unexpected O_2 affinity by the possible hydrogen bond with these specific NH groups. Indeed, these hydrogen-bond donors could be located in a position more favorable to a strong stabilization of the dioxygen adduct. In this paper, owing to the investigation of a series of tren-capped iron(II) porphyrins, differing by various substitutions on one or two amino functions, and the X-ray structure of such a tren-capped porphyrin, we show that the effect of the tripodal cage remains predominant versus the peripheral groups around the distal pocket. However, we also demonstrate that a group such as a nitrophenol, when appropriately attached at the periphery of the distal cage, can dramatically effect the dioxygen affinity by a factor up to 10^4, and so electrostatic repulsions can strongly destabilize the oxygenated complex without having a significant influence on the CO complex, which is more sensitive to steric effects.

Experimental Section

Materials and Methods. All commercial chemicals (Aldrich, Acros) and solvents (ACS for analysis) were used without further purification unless otherwise stated. Solvents used in an inert atmosphere (drybox; $[O_2] < 1$ ppm) were freshly distilled and deoxygenated by three "freeze−pump" cycles. Benzene, toluene, and THF were distilled over potassium benzophenone ketyl; methylene chloride, pyridine, triethylamine, and pentane were distilled over CaH_2; and methanol was distilled over magnesium turnings. Column chromatographies were performed on SiO_2 (Merck TLC−Kieselgel 60H, 15 μm). Mass spectra (EI, Varian MAT 33 spectrometer; ESI, Micromass MS/MS ZABSpec TOFF spectrometer) were performed at the C.R.M.P.O. (University of Rennes 1). ^{1}H and ^{13}C NMR spectra were recorded on a Bruker Avance 500 or Bruker Avance 300 spectrometer equipped with a TBI probe or a Bruker Avance 300 spectrometer with a BBO probe. Spectra were referenced with residual solvent protons. UV−vis spectra were recorded on an Uvikon XL spectrometer.

Equilibrium Measurements. The O_2, CO affinities were measured spectrophotometrically under equilibrium conditions with an Uvikon XL spectrometer. Measurements were performed with toluene solutions thermostated in the spectrometer to 25.0 ± 0.3 °C with a Lauda RL6 constant-temperature bath and circulator.

The equilibrium between the metalloporphyrin (MP) with an excess of axial base (B)—or an intramolecular fifth ligand—and O_2 can be expressed as follows

$$MP{\cdot}B + O_2 \overset{K}{\rightleftharpoons} MP{\cdot}B{\cdot}O_2$$

The equilibrium constant K is defined by

$$K = [MP{\cdot}B{\cdot}O_2]/[MP{\cdot}B]p(O_2)$$

If C_0 is the total concentration of (MP·B), then at $t = 0$ (without dioxygen) $C_0 = [MP{\cdot}B]$. At a t instant with a dioxygen partial pressure ($p(O_2)$), $C_0 = [MP{\cdot}B] + [MP{\cdot}B{\cdot}O_2]$. Then

$$K = [MP{\cdot}B{\cdot}O_2]/((C_0 - [MP{\cdot}B{\cdot}O_2]){\cdot}p(O_2))$$

Only (MP·B) and (MP·B·O_2) have absorbance in the UV−vis. The Beer−Lambert law can be written as follows.

When $t = 0$

$$A_o = \epsilon_{MP{\cdot}B}{\cdot}C_o = \epsilon_{MP{\cdot}B}[MP{\cdot}B] + \epsilon_{MP{\cdot}B}[MP{\cdot}B{\cdot}O_2]$$

and at any t

$$A = \epsilon_{MP{\cdot}B}[MP{\cdot}B] + \epsilon_{MP{\cdot}B{\cdot}O2}[MP{\cdot}B{\cdot}O_2]$$

Then

$$A - Ao = (e_{MP{\cdot}B{\cdot}O_2} - \epsilon_{MP{\cdot}B})[MP{\cdot}B{\cdot}O_2] \text{ or } \Delta A = \Delta\epsilon[MP{\cdot}B{\cdot}O_2]$$

The equilibrium constant K could be defined by

$$K = \Delta A/((C_0\Delta\epsilon - \Delta A){\cdot}p(O_2)) \text{ or } K^{-1} = ((C_0\Delta\epsilon/\Delta A){\cdot}p(O_2)) - p(O_2)$$

The partial pressure of dioxygen ($p(O_2)$) could be defined as $p(O_2) = ((C_0\Delta\epsilon/\Delta A){\cdot}p(O_2)) - K^{-1}$.

This is the equation of a straight line with a slope of $C_0\Delta\epsilon$ and an intercept of $-1/K$. When the metalloporphyrin is half-oxygenated, $[MP{\cdot}B] = [MP{\cdot}B{\cdot}O_2]$, then $1/K = P_{1/2}(O_2)$. The partial pressure of oxygen at which 50% of metalloporphyrin sites are bound with O_2 is defined as $P_{1/2}(O_2)$.

The reversibility of gas binding was monitored afterward by bubbling argon through the tonometer and recording several UV−vis spectra. However, since the affinity for dioxygen is very high, it was difficult to obtain the original absorption of the five-coordinate UV−vis spectrum due to solvent evaporation. As the reaction is very slow, the UV−vis spectrum of the dioxygen adduct was recorded after at least a week to verify that the absorption was not modified and hence that the equilibrium was actually reached.

Synthesis and Characterization. *meso*-α-5,10,15,20-Tetrakis-(2-acryloylamino)phenylporphyrin (α,α,α,α Michael acceptor) was prepared as described in the literature.[23]

***meso*-α-5,10,15,20-Tetrakis{2-[3,3′,3″3‴-{*N*,*N*,*N*′,*N*″-tris(2-aminoethyl)amino}tetrapropionylamino]phenyl}porphyrin, 1H$_2$.** To a solution of α,α,α,α Michael acceptor (2.5 g, 2.8 mmol) in chloroform/methanol (1/5) mixture (600 mL) degassed with Ar at

(16) Collman, J. P.; Herrmann, P. C.; Fu, L.; Eberspacher, T. A.; Eubanks, M.; Boitrel, B.; Hayoz, P.; Zhang, X. M.; Brauman, J. I.; Day, V. W. *J. Am. Chem. Soc.* **1997**, *119*, 3481−3489.

(17) Golberg, D. E. *Chem. Rev.* **1999**, *99*, 3371−3378.

(18) (a) Collman, J. P.; Fu, L.; Zingg, A.; Diederich, F. *Chem. Commun.* **1997**, 193−194. (b) Weyermann, P.; Diederich, F. *J. Chem. Soc., Perkin Trans. 1* **2000**, 4231−4233. (c) Zingg, A.; Felber, B.; Gramlich, V.; Fu, L.; Collman, J. P.; Diederich, F. *Helv. Chim. Acta* **2002**, *85*, 333−351.

(19) Ricard, D.; Andrioletti, B.; Boitrel, B.; Guilard, R. *New J. Chem.* **1998**, *22*, 1331−1332.

(20) Andrioletti, B.; Boitrel, B.; Guilard, R. *J. Org. Chem.* **1998**, *63*, 1312−1314.

65 °C for 1 h was added tris(2-aminoethyl)amine (465 μL, 3.1 mmol). The mixture was stirred for 2 days; then solvent was removed under vacuum. The resulting powder was dissolved in CH_2Cl_2/NH_3(g) and directly loaded on a silica gel chromatography column. The expected compound eluted with 4% MeOH/CH_2Cl_2/NH_3(g) was obtained in 68% yield (1.96 g). ^{1}H NMR (pyridine-d_5, 323 K): δ 11.42 (s, 2H, −NHCO); 9.17 (s, 2H, −NHCO), 9.08 (d, 2H, J = 4.5 Hz, $H_{\beta pyr}$); 9.06 (m, 2H, H_{aro}); 9.02 (d, 2H, J = 5.0 Hz, $H_{\beta pyr}$); 8.96 (s, 2H, $H_{\beta pyr}$); 8.81 (m, 4H, H_{aro} + $H_{\beta pyr}$); 8.09 (d, 2H, J = 6.5 Hz, H_{aro}); 7.87 (t, 2H, J = 7.5 Hz, H_{aro}); 7.83 (t, 2H, J = 7.5 Hz, H_{aro}); 7.77 (d, 2H, J = 7.5 Hz, H_{aro}); 7.55 (t, 2H, J = 7.0 Hz, H_{aro}); 7.46 (t, 2H, J = 7.0 Hz, H_{aro}); 2.35−2.12 (m, 10H); 2.09−1.99 (m, 4H); 1.86−1.80 (m, 2H); 1.09 (m, 2H); 0.84 (m, 2H); 0.70 (m, 2H); 0.47 (m, 2H); 0.01 (m, 2H); −0.13 (m, 2H); −1.57 (m, 2H); −2.29 (s, 2H, $-NH_{pyr}$). HR-MS (LSIMS-MS): calcd m/z = 1037.4939 for $C_{62}H_{61}N_{12}O_4$ $[M + H]^+$, found 1037.4929. UV−vis (CH_2Cl_2) λ, nm (10^{-3} ϵ, dm^3 mol^{-1} cm^{-1}): 421 (180.4); 515 (9.0); 548 (3.1); 588 (3.4); 644 (1.8). Anal. Calcd for $C_{62}H_{60}N_{12}O_4 \cdot 2H_2O$: C, 69.38; H, 6.01; N, 15.66. Found: C, 68.81; H, 5.54; N, 15.79.

Nickel(II) *meso*-α-5,10,15,20-Tetrakis{2-[3,3′,3″3‴-{*N*,*N*,*N*′,*N*″-tris(2-aminoethyl)amino}tetrapropionylamino]phenyl}-porphyrin, 2. To a solution of porphyrin $1H_2$ (0.539 mmol, 500 mg) in DMF (40 mL) was added nickel chloride (2.70 mmol, 350 mg). The mixture was stirred 3 h at 80 °C; then solvent was removed under vacuum. The resulting powder was dissolved in $CHCl_3/NH_3$(g) and directly loaded on a silica gel chromatography column. The expected compound was eluted with 0.8% MeOH/$CHCl_3/NH_3$(g) and obtained in 70% yield (412 mg). ^{1}H NMR (500.13 MHz, DMSO-d_6, 333 K): δ 11.11 (br s, 2H, −NHCO); 9.10 (s, 2H, −NHCO); 8.71 (s, 4H, $H_{\beta pyr}$); 8.65 (s, 2H, $H_{\beta pyr}$); 8.61 (d, 2H, ^3J = 8.2 Hz, H_{aro}); 8.49 (s, 2H, $H_{\beta pyr}$); 8.26 (d, 2H, J = 8.2 Hz, H_{aro}); 7.81 (m, 4H, H_{aro}); 7.73 (td, 2H, ^3J = 8.7 Hz and ^4J = 1.5 Hz, H_{aro}); 7.51 (t, 2H, J = 7.4 Hz, H_{aro}); 7.39 (d, 2H, J = 7.4 Hz, H_{aro}); 7.33 (td, 2H, ^3J = 7.4 Hz and ^4J = 0.8 Hz, H_{aro}); 2.14 (br m, 2H, $-CH_2-$); 2.04 (br m, 2H, $-CH_2-$); 1.98 (br m, 4H, $-CH_2-$); 1.82 (br m, 4H, $-CH_2-$); 1.67 (br m, 2H, $-CH_2-$); 0.95 (br s, 2H, $-CH_2-$); 0.71 (br s, 2H, $-CH_2-$); 0.61 (br m, 4H, $-CH_2-$); 0.38 (br s, 2H, $-CH_2-$); 0.16 (br m, 2H, $-CH_2-$); −0.90 (br s, 2H, $-CH_2-$). HR-MS (ESI-MS): calcd m/z = 1093.4135 for $C_{62}H_{59}N_{12}O_4{}^{58}Ni$ $[M + H]^+$, found 1093.4128 (1 ppm). UV−vis (CH_2Cl_2) λ, nm (10^{-3} ϵ, dm^3 mol^{-1} cm^{-1}): 415.0 (288.6); 526.5 (23.4); 559.5 (7.5).

***meso*-α-5,10,15,20-Tetrakis{2-[3,3′,3″3‴-{*N*,*N*,*N*′,*N*″-tris(2-aminoethyl)amino}-(*N*′,*N*″-bis-ethoxycarbonylmethyl)-tetrapropionylamino]phenyl}porphyrin, $3H_2$.** In a two-neck round-bottom flask equipped with a stir bar and gas inlet porphyrin $1H_2$ (202 mg, 0.195 mmol) was charged with THF (80 mL) and Et_3N (275 μL, 1.9 mmol). The reaction mixture was heated to 65 °C; then ethyl bromoacetate (194 μL, 1.75 mmol) was added dropwise. The solution was stirred for 2 days, and solvent was removed under vacuum. The resulting oil was precipitated with a THF/pentane (1/5) mixture and then dissolved with $CHCl_3$ and evaporated. The resulting powder was dissolved in $CHCl_3$ and directly loaded on a silica gel chromatography column. The expected compound was eluted with 2% MeOH/$CHCl_3$ and obtained in 64% yield (151 mg). ^{1}H NMR ($CDCl_3$, 323 K): δ 9.76 (s, 2H, −NHCO); 8.92 (d, 2H, J = 5.0 Hz, $H_{\beta pyr}$); 8.89 (d, 2H, J = 4.7 Hz, $H_{\beta pyr}$); 8.84 (s, 2H, $H_{\beta pyr}$); 8.70 (s, 2H, $H_{\beta pyr}$); 8.66 (d, 2H, J = 8.5 Hz, H_{aro}); 8.57 (d, 2H, J = 8.5 Hz, H_{aro}); 8.07 (s, 2H, −NHCO); 8.02 (dt, 2H, ^3J = 7.5 Hz and ^4J = 1.0 Hz, H_{aro}); 7.86 (td, 2H, ^3J = 8.0 Hz and ^4J = 1.5 Hz, H_{aro}); 7.81 (td, 2H, ^3J = 8.0 Hz and ^4J = 1.5 Hz, H_{aro}); 7.52 (m, 4H, H_{aro}); 7.37 (td, 2H, ^3J = 7.5 Hz and ^4J = 1.0 Hz, H_{aro}); 3.92 (q, 4H, J = 7.0 Hz, $-CH_{2\ ester}$); 2.58 (d, 2H, J = 16.5 Hz, $-CH_2$); 2.51 (m, 2H); 2.37 (m, 2H); 2.12 (m, 4H); 2.01 (m, 2H); 1.86 (m, 2H); 1.70 (m, 4H); 1.10 (t, 6H, J = 7,5 Hz, $-CH_3$); 0.91 (m, 2H); 0.66 (m, 4H); 0.55 (m, 4H); −1.72 (m, 4H); −2.55 (s, 2H, $-NH_{pyr}$). HR-MS (ESI-MS): calcd m/z = 1209.5674 for $C_{70}H_{73}N_{12}O_8$ $[M + H]^+$, found 1209.5678. UV−vis (CH_2Cl_2) λ, nm (10^{-3} ϵ, dm^3 mol^{-1} cm^{-1}): 421 (271.1); 514 (16.7); 547 (5.1); 588 (6.0); 645 (2.2). Anal. Calcd for $C_{70}H_{72}N_{12}O_4$: C, 69.52; H, 6.00; N, 13.90. Found: C, 69.21; H, 6.07; N, 13.81.

***meso*-α-5,10,15,20-Tetrakis{2-[3,3′,3″3‴-{*N*,*N*,*N*′,*N*″-tris(2-aminoethyl)amino}-(*N*′,*N*″-bis-3-ethoxycarbonyl-propionylamino)-tetrapropionylamino]phenyl}porphyrin, $4H_2$.** In a round-bottom flask equipped with a stir bar and gas inlet porphyrin $1H_2$ (100 mg, 0.09 mmol) was charged with THF (50 mL) and Et_3N (200 μL, 1.4 mmol). Ethyl succinyl chloride (55 μL, 0.38 mmol) was added dropwise. The solution was stirred for 12 h; then solvent was removed under vacuum. The resulting powder was dissolved in $CHCl_3$ and directly loaded on a silica gel chromatography column. The expected compound was eluted with 1.5% MeOH/$CHCl_3$ and obtained in 88% yield (100 mg). ^{1}H NMR (DMSO-d_6, 343 K): δ 9.67 (s, 2H, −NHCO); 8.77 (s, 2H, −NHCO); 8.69 (d, 2H, J = 4,5 Hz, $H_{\beta pyr}$); 8.62 (d, 2H, J = 4,5 Hz, $H_{\beta pyr}$); 8.52 (s, 2H, $H_{\beta pyr}$); 8.49 (s, 2H, $H_{\beta pyr}$); 8.31 (d, 2H, J = 4.8 Hz, H_{aro}); 8.12 (d, 2H, J = 7.3 Hz, H_{aro}); 7.85 (m, 5H, H_{aro}); 7.75 (d, 1H, J = 7.3 Hz, H_{aro}); 7.59 (m, 4H, H_{aro}); 7.49 (t, 2H, J = 7.1 Hz, H_{aro}); 4.07 (q, 4H, J = 7,1 Hz, $-CH_2CH_3$); 3.21 (m, 4H); 2.60 (m, 4H); 2.39 (m, 6H); 2.20 (m, 2H); 2.07 (m, 2H); 1.64 (br s, 4H); 1.48 (m, 6H); 1.25 (t, 6H, J = 7.5 Hz, $-CH_2CH_3$); 0.47 (t, 2H, J = 9,3 Hz); −1.16 (br s, 2H); −1.34 (br s, 2H); −2.75 (s, 2H, $-NH_{pyr}$); −2.86 (br s, 2H). HR-MS (ESI-MS): calcd m/z = 1293.5885 for $C_{74}H_{77}N_{12}O_{10}$ $[M + H]^+$, found 1293.5888. UV−vis (CH_2Cl_2) λ, nm (10^{-3} ϵ, dm^3 mol^{-1} cm^{-1}): 420.0 (291.3); 512.0 (13.2); 545.5 (4.7); 586.0 (4.7); 622 (1.4).

***meso*-α-5,10,15,20-Tetrakis{2-[3,3′,3″3‴-{*N*,*N*,*N*′,*N*″-tris(2-aminoethyl)amino}-(*N*′-2-hydroxy-5-nitro-benzyl)tetra-propionylamino]phenyl}porphyrin, $5H_2$.** In a 100 mL round-bottom flask under argon, 200 mg (0.193 mmol) of $1H_2$, 2-bromomethyl-4-nitrophenol (53.6 mg, 0.231 mmol), and 0.2 mL of Et_3N were dissolved in 50 mL of freshly distilled THF. The solution was heated at 65 °C overnight and then dried under vacuum. The product was dissolved in chloroform and poured onto a silica gel column. The disubstituted compound was eluted first with 5.6% MeOH/$CHCl_3$ in 16.5% yield (38 mg) followed by compound $5H_2$ eluting with 6.4% MeOH/$CHCl_3$ in 66% yield (168 mg). ^{1}H NMR (DMSO-d_6, 363 K): δ 10.93 (br s, 1H, NH); 9.42 (br s, 1H); 9.24 (br s, 1H); 8.90 (d, 1H, J = 5.0 Hz, $H_{\beta pyr}$); 8.89 (d, 1H, J = 4.5 Hz, $H_{\beta pyr}$); 8.79 (d, 1H, J = 5.0 Hz, $H_{\beta pyr}$); 8.76 (d, 1H, J = 5.0 Hz, $H_{\beta pyr}$); 8.69 (br s, 1H); 8.67 (d, 1H, J = 4.5 Hz, $H_{\beta pyr}$); 8.63 (d, 1H, J = 4.5 Hz, $H_{\beta pyr}$); 8.55 (d, 1H, J = 4.5 Hz, $H_{\beta pyr}$); 8.51 (d, 1H, J = 4.5 Hz, $H_{\beta pyr}$); 8.24 (dd, 1H, ^3J = 7.5 Hz and ^4J = 1.5 Hz, H_{aro}); 8.01 (d, 1H, J = 8.0 Hz, H_{aro}); 7.97 (d, 1H, J = 8.0 Hz, H_{aro}); 7.90 (dd, 1H, ^3J = 9.0 Hz and ^4J = 3.0 Hz, H_5); 7.87 (td, 1H, ^3J = 7.5 Hz and ^4J = 1.5 Hz, H_{aro}); 7.84 (d, 1H, J = 3.0 Hz, H_3); 7.83−7.75 (overlapping m, 6H, H_{aro}); 7.70 (td, 1H, ^3J = 7.5

(21) (a) Larsen, N. G.; Boyd, P. D. W.; Rodgers, S. J.; Wuenschell, G. E.; Koch, C. A.; Rasmussen, S.; Tate, J. R.; Erler, B. S.; Reed, C. A. *J. Am. Chem. Soc.* **1986**, *108*, 6950−6960. (b) Collman, J. P.; Bröring, M.; Fu, L.; Rapta, M.; Schwenninger, R.; Straumanis, A. *J. Org. Chem.* **1998**, *63*, 8082−8083.

(22) (a) Ricard, D.; Andrioletti, B.; L'Her, M.; Boitrel, B. *Chem. Commun.* **1999**, 1523−1524. (b) Ricard, D.; L'Her, M.; Richard, P.; Boitrel, B. *Chem. Eur. J.* **2001**, *7*, 3291−3297.

(23) Collman, J. P.; Zhang, X.; Herrmann, P. C.; Uffelman, E. S.; Boitrel, B.; Straumanis, A.; Brauman, J. I. *J. Am. Chem. Soc.* **1994**, *116*, 2681−2682.

Hz and ^4J = 1.5 Hz, H_{aro}); 7.64 (td, 1H, ^3J = 7.5 Hz and ^4J = 1.5 Hz, H_{aro}); 7.71 (d, 1H, J = 6.5 Hz, H_{aro}); 7.48 (td, 1H, ^3J = 7.5 Hz and ^4J = 1.5 Hz, H_{aro}); 7.45 (td, 1H, ^3J = 7.5 Hz and ^4J = 1.5 Hz, H_{aro}); 7.41 (td, 1H, ^3J = 7.5 Hz and ^4J = 1.5 Hz, H_{aro}); 7.64 (td, 1H, ^3J = 7.5 Hz and ^4J = 1.5 Hz, H_{aro}); 6.77 (d, 2H, J = 9.0 Hz, H_6); 3.18 (s, 2H, CH_{2benz}); 2.43 (m, 1H, $-CH_2-$); 2.24 (m, 1H, $-CH_2-$); 2.10−1.75 (overlapping m, 7H, $-CH_2-$); 1.62 (m, 4H, $-CH_2-$); 1.18 (m, 2H, $-CH_2-$); 0.87 (m, 2H, $-CH_2-$); 0.72 (m, 1H, $-CH_2-$); 0.5 (m, 1H, $-CH_2-$); −0.08 (m, 1H, $-CH_2-$); −0.22 (m, 1H, $-CH_2-$); −0.48 (m, 2H, $-CH_2-$); −0.58 (m, 1H, $-CH_2-$); −1.14 (m, 1H, $-CH_2-$); −1.20 (m, 1H, $-CH_2-$); −1.63 (m, 1H, $-CH_2-$); −2.45 (m, 1H, $-CH_2-$); −2.57 (s, 2H, $-NH_{pyr}$). HR-MS (ESI-MS): calcd m/z = 1188.5208 for $C_{69}H_{66}N_{13}O_7$ $[M + H]^+$, found 1188.5195. UV−vis ($CHCl_3$/MeOH 10%) λ, nm ($10^{-3}\epsilon$, $dm^3\ mol^{-1}\ cm^{-1}$): 423 (301.2); 517 (15.4); 550 (4.2); 589 (4.9); 645 (2.0).

***meso*-α-5,10,15-Tris{2-(3,3′,3″-[*N*,*N*′,*N*″-tris(2-aminoethylamino)propionylamino]triphenyl}-α-20-(2-methylaminophenyl)porphyrin, 6H$_2$.** The atropisomer α,α,α,α of *meso*-5,10,15,20-tetrakis(2-amino)phenylporphyrin (TAPP) (1 g, 1.48 mmol) was singly acetylated by slow addition of acetyl chloride over 1 h (115 μL, 1.1 mmol) in dry THF (500 mL) at 0 °C in the presence of NEt_3 (210 μL, 3.0 mmol). Stirring was maintained 1 h after the addition, and the solution was dried by rotary evaporation. The resulting powder was dissolved in methylene chloride and washed twice with 50 mL of aqueous NaOH (5%). The organic phase was concentrated and poured on a 15 μm silica gel column (6 × 10 cm) prepared with methylene chloride. The desired product was eluted with a mixture of 1.25% MeOH/CH_2Cl_2 (490 mg, yield = 46%). The reaction of the three remaining amino groups with acryloyl chloride in dry THF, according to the original method, led to the corresponding picket porphyrin. This picket porphyrin was allowed to react with tren according to the same procedure described for 1H$_2$. The desired product 6H$_2$ was eluted with 4% MeOH/CH_2Cl_2. After evaporation to dryness, 234 mg of a purple powder was collected (yield = 37%). ^{1}H NMR (500 MHz, $CDCl_3$, 323 K): δ 11.31 (s, 1H, −NHCO), 10.78 (s, 2H, −NHCO), 8.93 (d, ^3J = 7.5 Hz, ^4J = 1.2 Hz, 2H, H_{aro}), 8.91 (d, ^3J = 5.0 Hz, 2H, $H_{\beta-pyr}$), 8.88 (d, ^3J = 5.0 Hz, 2H, $H_{\beta-pyr}$), 8.86 (d, ^3J = 8.0 Hz, 2H, H_{aro}), 8.85 (d, ^3J = 5.0 Hz, 2H, $H_{\beta-pyr}$), 8.76 (br s, 2H, $H_{\beta-pyr}$), 7.89 (m, 1H, H_{aro}), 7.83−7.79 (m, 5H, H_{aro}), 7.67 (d, ^3J = 7.7 Hz, ^4J = 1.5 Hz, 2H, H_{aro}), 7.51 (m, 1H, H_{aro}), 7.41−7.35 (m, 3H, H_{aro}), 7.27 (s, 1H, −NHCO), 2.12−1.95 (m, 12H, $-CH_2$), 1.30 (s, 3H, $-CH_3$), 0.95 (m, 2H, −NH), 0.71 (m, 2H, $-CH_2$), 0.62 (m, 2H, $-CH_2$), 0.24 (m, 2H, $-CH_2$), −0.16 (m, 2H, $-CH_2$), −1.04 (m, 2H, $-CH_2$), −1.25 (m, 3H, $-CH_2$ + −NH), −2.53 (s, 2H, NH_{pyr}). ^{13}C NMR (125 MHz, $CDCl_3$, 323K): δ 171.9, 171.8, 163.2, 139.8, 139.0, 137.2, 136.7, 135.8, 132.2, 131.6, 131.0, 130.3, 130.0, 122.9, 122.7, 122.2, 121.8, 117.5, 117.2, 115.5, 49.6, 47.2, 43.9, 43.3, 42.5, 41.2, 35.4, 34.8, 30.1. UV−vis (CH_2Cl_2) λ, nm ($10^{-3}\epsilon$; $dm^3\ mol^{-1}\ cm^{-1}$): 421 (221.7); 515 (11.8); 552 (3.0); 589 (3.2); 646 (1.3). HR-MS (LSIMS): calcd m/z = 1025.4939 for $C_{61}H_{61}N_{12}O_4$ $[M + H]^+$, found 1025.4915. Anal. Calcd for $C_{61}H_{60}N_{12}O_4 \cdot H_2O$: C, 70.22, H, 5.99, N, 16.12. Found: C, 69.96, H, 5.89, N, 16.44.

***meso*-α-5,10,15-Tris{2-(3,3′,3″-[*N*,*N*′,*N*″-tris(2-amino-ethylamino)propionylamino]triphenyl}-α-20-(2-hydroxy-5-nitrobenzylamino-phenyl)porphyrin, 7H$_2$.** In a 500 mL round-bottom flask under argon, 650 mg (0.708 mmol) of *meso*-5,10,15-tris(2-amino)phenyl-20-(2-trityl-amino)phenylporphyrin (4.0-TrTAPP)[21] and 1 mL of Et_3N were dissolved in 250 mL of freshly distilled THF; then acryloyl chloride (208 μL, 2.55 mmol) dissolved in 20 mL of THF was added dropwise at −50 °C over 10 min. Stirring was maintained for 10 min, and then the mixture was dried under vacuum. The residue was dissolved in 30 mL of CH_2Cl_2, and 3 mL of trifluoroacetic acid was added. After 2 h the mixture was washed twice with 10 mL of aqueous NaOH (5%). The organic phase was concentrated by rotary evaporation and poured onto a 15 μm silica gel column (3 × 10 cm). The resulting tris-acrylamidophenyl-monoaminophenyl picket porphyrin was eluted with 0.6% MeOH/CH_2Cl_2. After evaporation to dryness, 330 mg was collected (yield = 50%). Then, in a 50 mL round-bottom flask under argon, 140 mg of picket porphyrin, 2-hydroxybenzaldehyde (150 mg, 1.2 mmol) and trifluoroacetic acid (55 μL), was dissolved in acetonitrile. After it was stirred overnight at room temperature, $NaBH_3CN$ was added and the solution was stirred for an additional 4 h. Then the mixture was neutralized by NH_3(g) and dried under vacuum. The resulting powder dissolved in CH_2Cl_2 was loaded on a silica gel chromatography column. The desired product was eluted with 10% acetone/CH_2Cl_2, and after evaporation to dryness it was allowed to react with tren according to the same procedure of 6H$_2$. The desired product was dissolved in CH_2Cl_2, poured onto a 15 μm silica gel column, and eluted with 5−10% MeOH/CH_2Cl_2/NH_3-(g). After evaporation to dryness, 7H$_2$ was collected (yield = 26%). ^{1}H NMR (500 MHz, DMSO-d_6, 333 K): δ 10.95 (br s, 1H, −NH), 10.63 (br s, 2H, −NH), 8.78 (br s, 4H, $H_{\beta pyr}$), 8.73 (br s, 4H, $H_{\beta pyr}$), 8.65 (br s, 2H, H_{aro}), 8.42 (d, 2H, J = 8.5 Hz, H_{aro}), 8.02 (br s, 1H, H_3), 7.82 (td, 3H, J_o = 7.5 Hz, J_m = 1.5 Hz, H_{aro}), 7.79 (td, 1H, ^3J = 7.5 Hz, ^4J = 1.5 Hz, H_{aro}), 7.74 (m, 1H, H_5), 7.77−7.64 (m, 5H, H_{aro}), 7.48 (t, 3H, ^3J = 7.0 Hz, H_{aro}), 7.42 (t, 2H, ^3J = 6.5 Hz, H_{aro}), 7.22 (d, 2H, J = 8.5 Hz, H_{aro}), 7.11 (t, 2H, ^3J = 7.5 Hz, H_{aro}), 6.33 (br s, 2H, H_6), 4.19 (s, 2H, CH_2), 2.00−1.84 (m, 12H, $-CH_2-$), 0.21 (br s, 2H, $-CH_2-$), −0.17 (br s, 2H, $-CH_2-$), −0.43 (br s, 2H, $-CH_2-$), −0.81 (br s, 2H, $-CH_2-$), −1.05 (br s, 2H, $-CH_2-$), −1.59 (br s, 2H, $-CH_2-$), −2.67 (s, 2H, $-NH_{pyr}$). HR-MS (ESI-MS): calcd m/z = 1134.5102 for $C_{66}H_{64}N_{13}O_6$ $[M + H]^+$, found 1134.5114. UV−vis ($CHCl_3$/MeOH 10%) λ, nm ($10^{-3}\epsilon$, $dm^3\ mol^{-1}\ cm^{-1}$): 421 (261.4); 517 (16.4); 551 (3.7); 590 (4.9);646 (1.5).

***meso*-α-5,10,15-Tris{2-(3,3′,3″-[*N*,*N*′,*N*″-tris(2-amino-ethylamino)propionylamino]triphenyl}-α-20-(2-hydroxy-5-nitrobenzoylamino-phenyl)porphyrin, 8H$_2$.** In a 100 mL round-bottom flask under argon, 80 mg (0.096 mmol) of *meso*-α-5,10,15-tris(2-acryloylamino)phenyl-α-20-(2-amino)phenylporphyrin described for 7H$_2$, DCC (39 mg, 0.191 mmol), DMAP (1 mg, 0.01 mmol), and 2-hydroxy-5-nitrobenzoic acid (35 mg, 0,191 mmol) were dissolved in 10 mL of freshly distilled pyridine. Stirring was maintained overnight, and then the mixture was dried under vacuum. The product was dissolved in chloroform and poured onto a 15 μm silica gel column. The desired product was eluted with 0.7% MeOH/$CHCl_3$. After evaporation to dryness, 50 mg was collected (yield = 52%) and then allowed to react with tren according to the same procedure described for 1H$_2$. The desired product was dissolved in CH_2Cl_2, poured onto a 15 μm silica gel column, and eluted with 5−10% MeOH/CH_2Cl_2/NH_{3g}. After evaporation to dryness, 50 mg of 8H$_2$ was collected (yield = 49%). ^{1}H NMR (500 MHz, DMSO-d_6, 363 K): δ 11.03 (br s, 3H, NH), 8.75 (d, 4H, J = 4.5 Hz, $H_{\beta pyr}$), 8.73 (d, 2H, J = 4.8 Hz, $H_{\beta pyr}$), 8.71 (d, 2H, J = 4.8 Hz, $H_{\beta pyr}$), 8.67 (broad d, 2H, H_{aro}), 8.60 (d, 2H, J = 8.0 Hz, H_{aro}), 8.56 (d, 1H, J = 3.2 Hz, H_3), 7.83−7.45 (m, 4H, H_{aro}), 7.73 (dd, 1H, ^3J = 7.0 Hz, ^4J = 1.5 Hz, H_{aro}), 7.52 (dd, 2H, ^3J = 7.5 Hz, ^4J = 1.8 Hz, H_{aro}), 7.43 (td, 2H, ^3J = 7.5 Hz, ^4J = 1.8 Hz, H_{aro}), 7.37 (td, 2H, ^3J = 7.5 Hz, ^4J = 1.8 Hz, H_{aro}), 7.35 (dd, 1H, ^3J = 9.0 Hz, ^4J = 3.2 Hz, H_5), 5.38 (d, 2H, J = 9.0 Hz, H_6), 2.06 (m, 4H, CH_2), 1.88 (m, 2H, CH_2), 1.80 (m, 4H, CH_2), 1.66 (m, 2H, CH_2), 0.62 (t, 2H, J = 9.0 Hz, CH_2), −0.06 (t, 2H, J = 9.0 Hz, CH_2), −0.20 (m, 2H, CH_2), −0.36 (t, 2H, J = 9.0 Hz, CH_2), −1.23 (m,

2H, CH_2), −1.46 (m, 2H, CH_2), −2.52 (s, 2H, $-NH_{pyr}$). HR-MS (ESI-MS): calcd m/z = 1148.4895 for $C_{66}H_{62}N_{13}O_7$ $[M + H]^+$, found 1148.4877. UV−vis ($CHCl_3$/MeOH 10%) λ, nm (10^{-3} ϵ, $dm^3\ mol^{-1}\ cm^{-1}$): 423 (323.4); 519 (16.8); 550 (3.9); 590 (4.7); 646 (1.9).

***meso*-α-5,10,15-Tris{2-(3,3′,3″-[*N*,*N*′,*N*″-tris(2-amino-ethylamino)propionylamino]triphenyl}-*β*-20-(2-{3-[(pyridin-3-ylmethyl)amino]propionylamino}phenyl)porphyrin, 9H$_2$.** In a 100 mL round-bottom flask under argon atmosphere *meso*-α-5,10,15-*β*-20-tetrakis(2-acryloylamino)phenylporphyrin (α,α,α,*β* Michael acceptor) was prepared according to the usual method. The latter (1 g, 1.12 mmol) was dissolved in 600 mL of a $CHCl_3$/MeOH (1/5) mixture degassed for 2 h. The solution was heated at 55 °C, and then tris(2-aminoethyl)amine (170 μL, 1.13 mmol) was added in one portion with a syringe. The reaction mixture was stirred for 24 h, and 5 equiv of 3-aminomethylpyridine (305 μL, 5.65 mmol) was added in one portion. Stirring was maintained for 24 h, and then the mixture was dried under vacuum. The resulting powder was dissolved in dichloromethane and loaded on a silica gel chromatography column. The expected compound eluted with 4% MeOH/$CHCl_3$/NH_3(g) was obtained in 12% yield (160 mg). ^{1}H NMR (500 MHz, $CDCl_3$, 323 K): δ 11.27 (s, 1H), 10.96 (s, 2H), 9.31 (s, 1H), 8.95 (d, 2H, J = 8.5 Hz), 8.92 (d, 2H, J = 4.5 Hz), 8.86 (m, 8H), 8.68 (d, 1H, J = 8.5 Hz), 7.95 (dd, 1H, ^3J = 7.5 Hz, ^4J = 1.5 Hz), 7.89 (td, 2H, ^3J = 1.5 Hz, ^4J = 7.5 Hz), 7.83 (t, 3H, J = 7.5 Hz), 7.67 (d, 1H, J = 5.0 Hz), 7.59 (td, 3H, ^3J = 1.5 Hz, ^4J = 7.5 Hz), 7.40 (t, 3H, 7.5 Hz), 6.35 (s, 1H), 5.83 (dd, 1H, ^3J = 4.5 Hz, ^4J = 7.5 Hz), 4.50 (d, 1H, J = 7.5 Hz), 2.15−1.90 (m, 10H), 1.79 (t, 2H, J = 5.5 Hz), 1.69 (t, 2H, J = 5.5 Hz), 1.33 (m, 2H), 0.91 (t, 1H), 0.66 (m, 2H), 0.55 (br s, 2H), 0.37 (s, 2H), 0.21 (br s, 2H), −0.19 (br s, 2H), −0.13 (br s, 2H), −1.31(br s, 2H), −1.63 (br s, 2H), −2.67 (s, 2H). HR-MS (ESI): calcd m/z = 1145.5626 for $C_{68}H_{69}N_{14}O_4$ $[M + H]^+$, found 1145.5632. UV−vis ($CHCl_3$) λ, nm (10^{-3} ϵ, $dm^3\ mol^{-1}\ cm^{-1}$): 425 (453.7); 517 (18.6); 552 (4.9); 592 (5.5); 648 (1.8).

Iron(II)-Metalated 1. In a drybox, to a solution of porphyrin **1H$_2$** (10 mg, 0.01 mmol) in THF (6 mL) was added iron(II) bromide (20 mg, 0.1 mmol). The mixture was stirred overnight at 65 °C; then solvent was removed under vacuum. The resulting powder was dissolved in benzene/methanol (5/1) and directly loaded on a silica gel chromatography column. The expected compound was eluted with a gradient of methanol in benzene. HR-MS (LSIMS-MS): calcd m/z = 1091.4132 for $C_{62}H_{59}N_{12}O_4{}^{56}Fe$ $[M + H]^+$, found 1091.4160. UV−vis (toluene, 1000 equiv of 2-methylimidazole): λ_{max} 442 nm (Soret); $+O_2$ 420 nm.

Iron(II)-Metalated 3. The insertion of the iron(II) is carried out according to the procedure described for **1** in a drybox. HR-MS (ESI-MS): calcd m/z = 1285.4686 for $C_{70}H_{70}N_{12}O_8{}^{56}FeNa$ $[M + Na]^+$, found 1285.4671. UV−vis (toluene, 1000 equiv of 2-methylimidazole): λ_{max} 443 (Soret), 564 nm; $+O_2$ 424 nm.

Iron(II)-Metalated 4. The insertion of the iron(II) is carried out according to the procedure described for **1** in a drybox. HR-MS (ESI-MS): calcd m/z = 1400.5082 for $C_{75}H_{77}N_{12}O_{11}Na^{56}Fe$ $[M - OMe + Na]^+$, found 1400.5082. UV−vis (toluene, 1000 equiv of 2-methylimidazole): λ_{max} 439 (Soret), 564 nm; $+O_2$ 422 (Soret), 510 nm.

Iron(II)-Metalated 5. In a 100 mL round-bottom flask under argon, 86 mg (0.04 mmol) of iron(III) μ-oxodimer of **1**, 2-bromomethyl-4-nitrophenol (21.8 mg, 0.094 mmol), and 0.1 mL of Et_3N were dissolved in 20 mL of freshly distilled THF. The solution was heated at 65 °C overnight and then dried under vacuum. The resulting powder was dissolved in chloroform, washed with HCl (2 M), neutralized with saturated $NaHCO_3$, and dried over $MgSO_4$. After filtration and evaporation the resulting powder was dissolved in chloroform and poured onto a silica gel column. The disubstituted compound was eluted first with 8−12% MeOH/$CHCl_3$ followed by compound **5** eluted with 16% MeOH/$CHCl_3$ in 66% yield (53 mg). In a drybox, to a solution of porphyrin **5** (20 mg, 0.016 mmol) in $CHCl_3$ (4 mL) was added a solution of $Na_2S_2O_4$. The mixture was stirred 30 min at room temperature; then the organic layer was separated and dried over $MgSO_4$. After filtration and evaporation the resulting powder was dissolved in chloroform, and a large excess of 2-methylimidazole was added. The crude product was precipitated by addition of pentane, providing iron(II)-metalated **5**. HR-MS (ESI-MS): calcd m/z = 1277.4092 for $C_{69}H_{64}N_{13}O_7{}^{56}Fe^{35}Cl$ $[M + H]^+$, found 1277.4086. UV−vis (toluene, 1000 equiv of 2-methylimidazole): λ_{max} 444.5 (Soret), 564 nm; $+O_2$ 425 (Soret), 510 nm.

Iron(II)-Metalated 6. The synthesis is identical to that of **1**. HR-MS (LSIMS): calcd m/z = 1079.4132 for $C_{61}H_{59}N_{12}O_4Fe$ $[M + H]^+$, found 1079.4133.

Iron(II)-Metalated 7. The insertion of the iron(II) is carried out according to the procedure described for **5**. HR-MS (ESI-MS): calcd m/z = 1223.3984 for $C_{66}H_{62}N_{13}O_6{}^{56}Fe^{35}Cl$ $[M + H]^+$, found 1223.4019. UV−vis (toluene, 1000 equiv of 2-methylimidazole): λ_{max} 444 (Soret), 564 nm; $+O_2$ 425 (Soret), 510 nm.

Iron(II)-Metalated 8. The insertion of the iron(II) is carried out according to the procedure described for **5**. HR-MS (ESI-MS): calcd m/z = 1237.3779 for $C_{69}H_{65}N_{13}O_7{}^{56}Fe^{35}Cl$ $[M + H]^+$, found 1237.3783. UV−vis (toluene, 1000 equiv of 2-methylimidazole): λ_{max} 443 (Soret), 564 nm; $+O_2$ 422 (Soret), 510 nm.

Iron(II)-Metalated 9. In a drybox, to a solution of porphyrin **9H$_2$** (10 mg, 0.009 mmol) in THF (6 mL) was added iron(II) bromide. The mixture was stirred overnight at 65 °C; then solvent was removed under vacuum. The resulting powder was dissolved in benzene/MeOH (5/1) and directly loaded on a silica gel chromatography column. The expected compound was eluted with a gradient of methanol in benzene with triethylamine. HR-MS (ESI-MS): calcd m/z = 1198.4741 for $C_{68}H_{66}N_{14}O_4{}^{56}Fe$, found 1198.4745 $[M]^{+\bullet}$. UV−vis (toluene): λ_{max} 439 (Soret); + O_2 428 nm.

Results and Discussion

Although the series of porphyrins **1** and **3**−**9** were initially synthesized as bimetallic chelators able to hold a copper cation above iron in the porphyrin,[22] they were studied in this work as iron complexes, the tripodal cap remaining free of any metal. Indeed, owing to Collman congruent Michael addition,[23] we were able to obtain two different tren-capped porphyrins related to **1** and **6** (Figure 2).[20] In these two ligands the tren is attached to the porphyrin core by either four or three linkers, respectively. As previously reported for aza-crown-capped porphyrins,[16] the iron complexes of these tetraaza-tripodal ligands do not form a six-coordinate complex but remain five coordinate with a nitrogen base as pyridine or *N*-methyl imidazole. This observation is of paramount importance as five-coordinate porphyrin complexes are required for equilibrium measurements. In Figure 3 is represented the typical ^{1}H NMR spectrum of a S = 2 paramagnetic complex with the characteristic *β*-pyrrolic signals around 50−55 ppm.

In a preliminary study we noticed that **1** and **6** exhibited high affinities for dioxygen with $P_{1/2}$ values around 10^{-5} Torr.[19] It should be mentioned that such affinities for

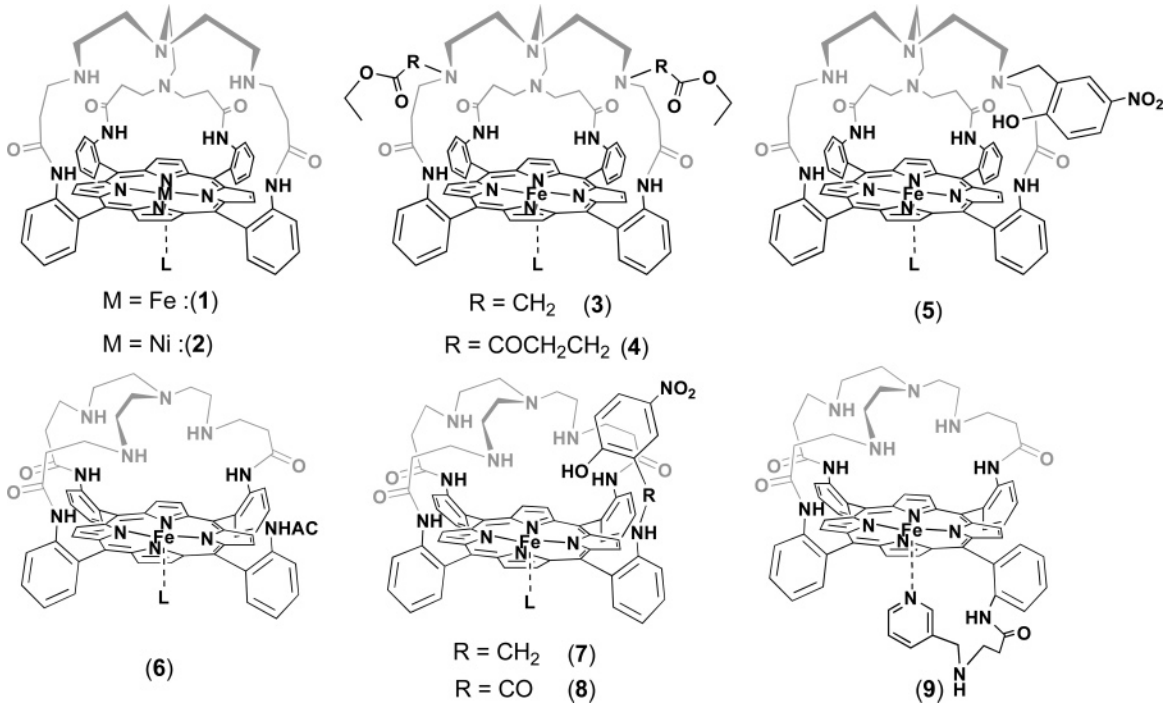

Figure 2. Chemical structure of the various compounds referred to in the text: L = 2-MeIm or 1,2-Me_2Im.

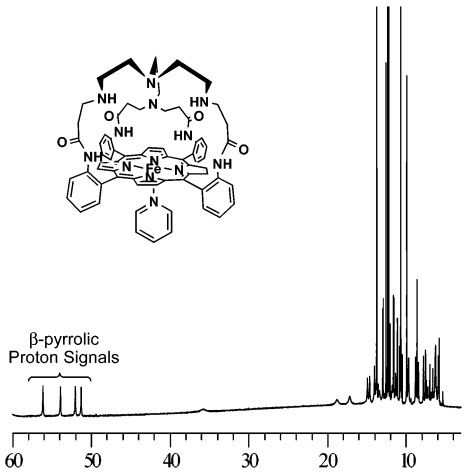

Figure 3. ^{1}H NMR spectra of O_2-free complex of compound **1** in pyridine-d_5.

dioxygen are by far too high to yield biomimetic dioxygen carriers. Consequently, it is crucial to determine the various features that could be able to modulate this affinity. Obviously, we have explained these affinities by a possible hydrogen bond with the secondary amines of the cap. This result has motivated the substitution of at least one amino function of the cap by various groups to obtain the family of eight iron porphyrins depicted in Figure 2. One can distinguish two distinct groups of porphyrins. The first one related to **1** in which the tetraaza-tripod is tethered by four links is composed of **3**, **4**, and **5** (first line, Figure 2). The second group related to **6** consists of various substitutions on one meso-aromatic ring of the porphyrin, as the tripod is attached by only three links in this group (second line, Figure 2). The dioxygen affinities have been measured as the $P_{1/2}$, according to the method exhaustively reported by Collman,[14] and are specified in Table 1 along with the carbon monoxide affinities as well as the resulting *M* values. Two striking observations have to be made. First, whatever the number of linkers between the tripodal cap and the porphyrin, the dioxygen affinities are about 10^2 higher than those reported for dendritic porphyrins.[18a] For the latter, a hydrogen bond engaged with an apical amide group—five atoms away from the meso-phenyl ring—has been proposed. As in our tren-capped complexes the secondary amines atom are located four atoms away from the meso-phenyl ring, they could be implied to be in a strong hydrogen bond with the terminal oxygen atom of the bound dioxygen. On the other hand, if these amine functions were the single factor able to influence the dioxygen affinity, the latter should not be as high as it is in the case of porphyrin **3** or **4**. Indeed, in these two last complexes the two secondary amines have been substituted by either an acetate or an ethyl succinate group for **3** or **4**, respectively. In both cases, the resulting tertiary amines or the secondary amides are not able to act as a donor in a hydrogen bond. Nevertheless, the measured $P_{1/2}$ are 2.4×10^{-5} and 2.7×10^{-4} Torr for **3** and **4**, respectively.

Although the affinity of the acyl-substituted compound **4** is 10-fold decreased, these results suggest that the dioxygen affinity is predominantly determined by the nature and structure of the cavity. In our case, the tetraaza-tripodal/tetrapodal structure is likely to determine the high dioxygen affinity.

The predominance of the distal cap is also significant in regard to the proximal base. Indeed, by comparing iron porphyrins **6** and **9**—which bears an internal nitrogen base and for which we have reported a one-pot two-step synthesis[24]—we note that the affinities for dioxygen are not very different. This second comparison is definitely in

(24) Even, P.; Ruzié, C.; Ricard, D.; Boitrel, B. *Org. Lett.* **2005**, *7*, 4325−4328.

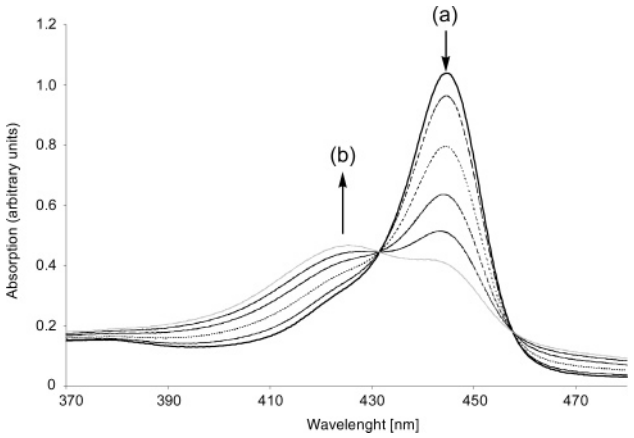

Figure 4. Typical data obtained for determination of $P_{1/2}(O_2)$ for **5** with 2-MeIm in CH_2Cl_2 at 25 °C: (a) under 1 atm of nitrogen; (b) under O_2 partial pressure of 8.27 Torr. Intermediate partial pressures of O_2: 0.059, 0.353, 1.235, and 3.291 Torr.

agreement with what was observed with the triaza-crown-capped porphyrins of Collman et al.[16] Incidentally, the binding of dioxygen on **9** led to a diamagnetic superoxo complex, as probed by its proton NMR spectrum ranging from 11 to 0 ppm, with poorly resolved signals.

On the other hand, a third comparison including porphyrins **5**, **7**, and **8** with porphyrin **1** results in a new conclusion. Indeed, it is striking that the $P_{1/2} = 0.675$ Torr value obtained for **5** (Figure 4) is not at all in the same range as all the others (Table 1). This measurement was carried out in methylene chloride and toluene but is much more difficult to carry out in toluene because the complex tends to precipitate in this solvent. Nevertheless, measurements of $P_{1/2}(O_2)$ in these two solvents show that they do not significantly effect the affinity of the complex for dioxygen.

However, it is known from the work of Reed et al.[15] that a phenol group, when located around the distal cage of a heme, should enhance its affinity for dioxygen (Figure 1, model b). One of the two secondary amines of porphyrin **5** has been alkylated by a benzyl nitrophenol moiety. The proton of the *p*-nitrophenol group is known to be acidic as the pK_a of the acido−basic couple phenol/phenate is around 7.5. In contrast to a phenol group, a possible explanation could be that the nitrophenol group would partially exist as the nitrophenate and thereby strongly destabilize the iron superoxo complex. Indeed, in complex **5** the "lateral arm" is expected to be flexible and the O atom of the phenol could point toward the inside of the cavity. Our molecular mechanics modeling show that this particular orientation of the hydroxy group inside the pocket is possible without any distortion of either the porphyrin core or the tripodal cap. This destabilization of the superoxo complex could explain the 10^4-fold decrease of the dioxygen affinity of iron complex **5** relative to iron complex **1**. So, why are the affinities of **7** and **8** not affected by the same factor as both of them also bear the same nitrophenol motif ? The main structural difference between **7**−**8** and **5** is the point of attachment of the phenol. Indeed, in **7** and **8** the phenol is grafted on an ortho position of the fourth meso-aromatic cycle. This particular geometry implies that the phenol is somehow facing the tren cap with the hydroxy group oriented inside the cavity, instead of being linked on it as in **5**. Additionally, we studied the conformation in solution of **7** and **8**.[25] On the ROESY spectrum of **8** (see Supporting Information, S19) in which the phenol is linked via an amide linkage it appears obvious that the OH group is indeed blocked between two lateral tren linkers. This orientation generates significant NOE on the corresponding methylene signals of either the linkers or the tren. The observation of the ROESY spectrum of **7** in which the phenol is linked via a benzyl linkage led to the conclusion that this specific orientation does not exist in **7** and that the nitrophenol hydroxy function is not oriented toward the center of the cavity. Thus, in porphyrins with the tren being tris-linked and when oriented toward the inside of the distal cage as in **8**, it is plausible that the phenol cannot be located close enough to the superoxo complex to destabilize it. Indeed, in this case the phenolic OH could be maintained away from the cavity by the presence of the tren itself. Therefore, the only predominant effect is the influence of the tripodal cap. On the other hand, in porphyrin **5**, in which the phenol is attached to the cap with the possibility to "dive" inside the distal cavity, the effect of the cap becomes negligible.

Obviously, the tetraaza composition of the cap has to be important for the gas binding interactions. However, our compounds do not behave as the aza-crown-capped porphyrins of Collman do toward the coordination of O_2 or CO[23] as, for instance, the cyclam-capped iron(II) porphyrin does not bind carbon monoxide at atmospheric pressure. This prompted us to also investigate the shape of the cap itself. As already mentioned above, by proton NMR spectroscopy we studied our capped tripodal porphyrins as free-base molecules in solution. We were able to perform the full assignment of the protons using a combination of standard 2D experiments such as COSY, TOCSY, heteronuclear H−C HSQC. The first comment concerns the high symmetry of the molecule as shown by the equivalence of the two branches of the tren surrounding the substituted phenol in **8**, for instance. Also remarkable is the strong high-field shift of all the resonances of the methylene protons of the tren.[25] This shielding must be related to a large movement of the tren toward the porphyrin plane. These conclusions were also confirmed by a single-crystal X-ray structural analysis of **2**, the nickel counterpart of **1**. Although nickel(II) cation is smaller than iron(II) cation[26] and is known to remain four coordinate in a square-planar geometry, the structure of **2** should be close to the structure of the six-coordinate oxygenated iron(II) complex **1**. Indeed, the nickel atom is expected to be located in the mean plane of the porphyrin as the iron atom in the case of a diamagnetic six-coordinate complex.[27] Nevertheless, due to O_2 or CO binding in the distal pocket, it should be mentioned that the cap itself can

(25) Gueyrard, D.; Didier, A.; Ruzié, C.; Bondon, A.; Boitrel, B. *Synlett* **2004**, 1158−1162.
(26) (a) Shannon, R. D.; Prewitt, C. T. *Acta Crystallogr.* **1969**, *B25*, 925. (b) Shannon, R. D. *Acta Crystallogr.* **1976**, *A32*, 751−767.
(27) (a) Bytheway, I.; Hall, M. B. *Chem. Rev.* **1994**, *94*, 639−658. (b) Lippard, S. J.; Berg, J. M. *Principles of Bioinorganic Chemistry*; University Science Books: Mill Valley, 1994.

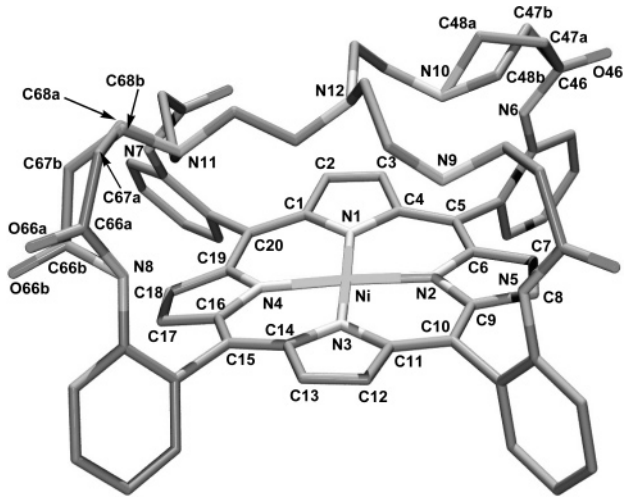

Figure 5. Stick drawing of the solid-state structure of compound **2**. Note that two of the four spacers are disordered over two positions.

adopt a different conformation in the six-coordinate iron(II) complex. X-ray-quality crystals of **2** were obtained by slow diffusion at room temperature of a mixture of acetonitrile/ethanol in an ethylenediamine solution of **2**. The nickel complex crystallized with both an ethanol molecule and an acetonitrile molecule surrounding it in the lattice.

Observing the stick drawing of **2** (Figure 5), it is evident that the tren cap is linked by four linkers as predicted by the proton NMR analysis. It is also clear that two diametrically opposed linkers are disordered. Structural refinement evidenced a light disorder in carbon and/or oxygen atoms in two of the four "O···N" pathways. One of them concerns only two carbon atoms (C47 and C48), where the second one is extended over four atoms (O66 oxygen atom and C66, C67, and C68 carbon atoms). Use of *PART* keyword in the SHELXL[28] refinement program allowed us to correctly describe this disorder (labeled as 'a' and 'b' pathways) and get realistic anisotropic displacement parameter values for these parts of the molecular structure. Attempts to refine the ratio of the different pathways has been realized but clearly indicated a 50−50 proportion for each of them. Final refinement has been performed with fixed and equal values of 'a' and 'b' pathways. Additionally, disorder has also been introduced in the modeling of the ethanol solvent molecule present in the asymmetric unit cell. The tetraaza-tripod is attached through its three primary amines to four pickets of the porphyrin. Thus, one nitrogen atom (N11) is linked to two pickets, where the two other nitrogen atoms (N9 and N10) are linked to only one picket each. We have taken advantage of this possible structure of the tren to obtain two different geometries of tren-capped porphyrins represented by **1** and **6**. To obtain the three linked series, different synthetic routes have been explored. The first one that we have chosen consists of opposing tren with a tris-acrylamide picket porphyrin to prepare **6**.[29] The second possibility is

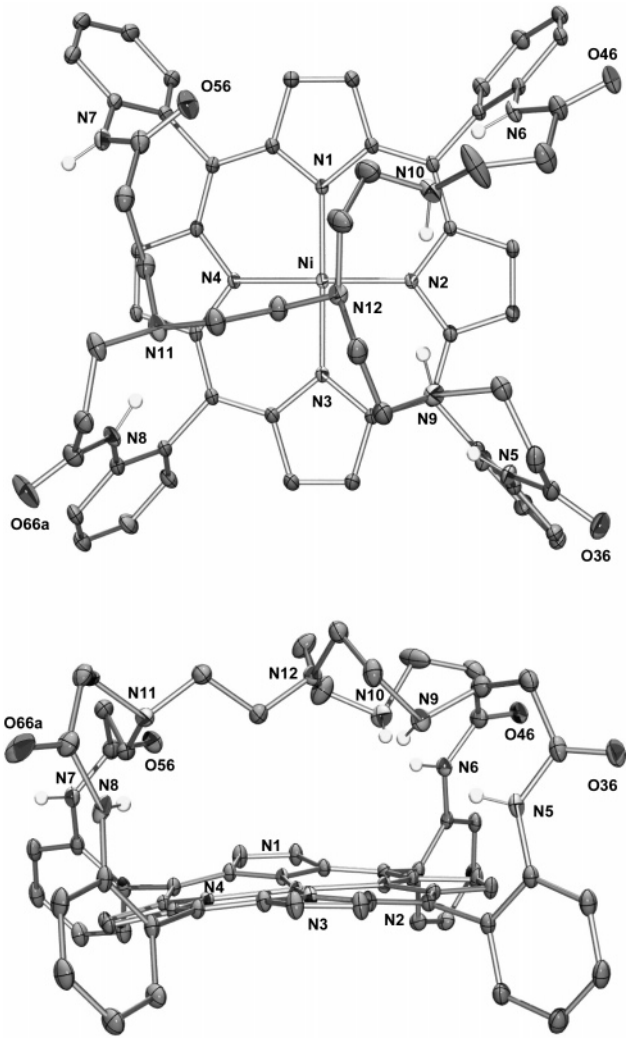

Figure 6. Thermal ellipsoid views (set to the 10% probability level) of the solid-state structure of compound **2** (top: apical view; bottom: side view). Solvent molecules are not represented.

illustrated by the reaction of a tris-alkylated tren on the tetrakis-acrylamide picket porphyrin.[30] Thus, when the tren is attached by four spacers, the resulting distal pocket is actually composed, on one hand, of two tertiary nitrogen atoms (N11 and N12), one of them being the tripodal nitrogen atom, and, on the other hand, of two secondary nitrogen atoms (N9 and N10). The latter are midway between a lateral location as are N5, N6, N7, and N8 and an apical site as is N12 (Figure 6). It is worth mentioning that in this solid-state structure all the N−H dipoles are oriented toward the inside of the cavity but N7, incorporated in one of the four meso-amide linkages.

Thus, these N−H dipoles are potential candidates as hydrogen-bond donors. Incidentally, the two secondary nitrogen atoms N9 and N10 from the tripod are each included in a short hydrogen bond with N5 and N6, respectively, but in these hydrogen bonds N9 and N10 act as acceptors with an acceptor to donor distance between d(N10−N6) = 2.741

(28) Sheldrick, G. M. *SHELXS and SHELXL*, Programs for Crystal Structure Analysis (Release 97-2); Institut für Anorganische Chemie der Universität: Göttingen, Germany, 1998.

(29) Didier, A.; L'Her, M.; Boitrel, B. *Org. Biomol. Chem.* **2003**, *1*, 1274−1276.

(30) (a) Baeg, J. O.; Holm, R. H. *Chem. Commun.* **1998**, 571−572. (b) Collman, J. P.; Fu, L.; Herrmann, P. C.; Wang, Z.; Rapta, M.; Bröring, M.; Schwenninger, R.; Boitrel, B. *Angew. Chem., Int. Ed. Engl.* **1998**, *37*, 3397−3400.

Å and d(N9−N5) = 2.776 Å. Apparently, in solution this observation implies that the N−H dipoles from N9 and N10 could also act as a hydrogen-bond donor with the oxygenated complex. A third weaker intermolecular hydrogen bond exists between the amide N7 and the amide O46 with a distance of 2.996 Å. The three secondary nitrogen atoms of the tripod form a plane with an angle of 4.53° with the least-squares mean plane of the porphyrin. These two planes are separated by a distance of 3.53 Å, and the tertiary nitrogen atom N12 is located 0.85 Å above the N9,N10,N11 plane and, so, 4.38 Å above the mean porphyrin plane. These distances can be compared with those reported for the unique X-ray structure of a cyclic triaza-crown-capped porphyrin.[31] For this triaza-cyclononane-capped zinc(II) porphyrin the distance between the mean porphyrinic plane and the triazacycle is 3.97 Å and the angle between the two planes is 5.75°. Although the distance between the two planes is smaller in our system, the tren is much more flexible with distances between the nitrogen atoms also greater than in the case of the triazacyclononane. Additionally, the nitrogen atom located at the top of the cap is not tightly bound in a rigid cyclic structure.

This may explain why these tren-capped iron(II) porphyrins, from a general point of view, do not discriminate carbon monoxide versus dioxygen in the range that could be expected. However, while observing the $P_{1/2}$(CO) column, a trend tends to emerge from Table 1. Definitely, the three-linked tren-capped iron(II) complexes **6**−**9** exhibit affinities for CO which are at least 10^2 higher than those measured for complexes **1** and **3**−**5** in which the cap is four-linked to the porphyrin. This observation is consistent with a stronger steric hindrance of the tripodal cap in the complexes in which the center of the tripod is almost in an apical position to the metal in the porphyrin (Figure 6, top view). On the other hand, in complexes **6**−**9** the tren motif being only three-linked to the porphyrin is clearly expected to be off-centered relative to the apical position to the iron and hence should not exhibit a strong influence on CO binding. Furthermore, one can verify that the affinity of **5** for CO is 10-fold lower than it is for **1**, for instance. This led to a discrimination factor M around 100 instead of 1 for the other complexes of this study. However, it should be emphasized that this increase of M is mostly due to the decrease of affinity for O_2 binding. Nevertheless, this small decrease of the CO affinity is explainable either by an additional and direct steric effect of the nitrophenol residue on the bound CO or to a change of conformation of the tren cap due to substitution by a nitrophenol group. However, it is difficult to choose between these two different hypotheses in the absence of an X-ray structure of ligand **5H₂** or one of its metalated derivatives. In summary, it is worth noting that these tren-capped iron(II) porphyrins exhibit high affinities for both dioxygen and CO. Indeed, in only one example for which the dioxygen adduct is destabilized due to the nitrophenol residue the M value reaches 100. This can be explained as the X-ray structure of **2** indicates that the tripodal nitrogen atom cannot induce any steric hindrance to the linear bound CO.

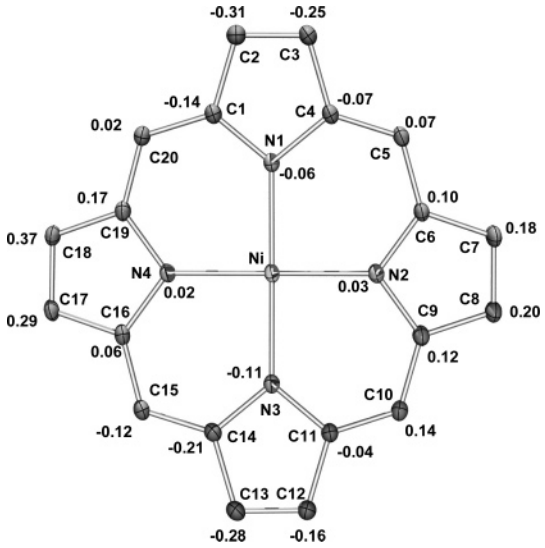

Figure 7. Distances of the 24 atoms from the mean plane of nickel porphyrin **2**.

Surprisingly, the porphyrinic core of **2** is not as distorted as it is expected to be. Indeed, nickel(II) porphyrins are usually deformed in a ruffled geometry.[32] The average Ni−N bond length is 1.945 Å and compares with other severely ruffled nickel(II) porphyrins for which this distance is 1.921 Å.[33,34] On the other hand, the torsion angle between two opposite pyrroles is very often an accurate criterion to evaluate the degree of distortion in ruffled porphyrins. For instance, it can rise in value up to 37° in bis-strapped porphyrins. However, in the X-ray structure of **2** this torsion (C2, C3, C12, C13) is only 2.46°. In fact, the distortion observed in **2** is more related to a saddle shape than a ruffle shape as it should be.

In the saddle shape, and as depicted in Figure 7, the two pairs of opposite pyrroles are located on each side of the porphyrin: N1−C1−C2−C3−C4 and N3−C11−C12−C13−C14 below the mean porphyrin plane where N2−C6−C7−C8−C9 and N4−C16−C17−C18−C19 are above the latter. Again, it appears that the predominance of the cap influences not only the affinity of dioxygen or carbon monoxide, but also the distortion of the porphyrin plane itself.

Conclusion

From this work we showed that arbor porphyrins capped with a tetraaza tripod exhibit remarkable affinities for dioxygen. To know if these unusual dioxygen affinities are due to the presence of secondary amine group donors of

(31) Collman, J. P.; Schwenninger, R.; Rapta, M.; Bröring, M.; Fu, L. *Chem. Commun.* **1999**, 137−138.

(32) (a) Sparks, L. D.; Medforth, C. J.; Park, M. S.; Chamberlain, J. R.; Ondrias, M. R.; Senge, M. O.; Smith, K. M.; Shelnutt, J. A. *J. Am. Chem. Soc.* **1993**, *115*, 581−592. (b) Jentzen, W.; Simpson, M. C.; Hobbs, J. D.; Song, X.; Ema, T.; Nelson, N. Y.; Medforth, C. J.; Smith, K. M.; Veyrat, M.; Mazzanti, M.; Ramasseul, R.; Marchon, J. C.; Takeuchi, T.; Goddard, W. A.; Shelnutt, J. A. *J. Am. Chem. Soc.* **1995**, *117*, 11085−11097.

(33) Richard, P.; Rose, E.; Boitrel, B. *Inorg. Chem.* **1998**, *37*, 6532−6534.

(34) Tani, F.; Matsu-ura, M.; Ariyama, K.; Setoyama, T.; Shimada, T.; Kobayashi, S.; Hayashi, T.; Matsuo, T.; Hisaeda, Y.; Naruta, Y. *Chem. Eur. J.* **2003**, *9*, 862−870.

hydrogen bond in the distal cage itself these amine functions were substituted in a systematic way by various groups. The latter were shown not to have a significant effect on the affinity of the iron complex for dioxygen except for only one model. Indeed, if one of the secondary amine functions of the tripod carries an electron-withdrawing group as a *p*-nitrophenol, the stability of the oxygenated complex is decreased by a factor 10^4. We propose, to explain this remarkable effect, that the phenol is in fact in the form of phenate due to the acidity of the phenolic proton. Thus, the stability of the phenate group reinforced by the nitro group in the para position destabilizes in a clear way the oxygenated complex by means of electrostatic repulsion.

On the other hand, if this same group is attached to one of the aromatic cycles in a meso position, it remains without effect on the stability of the oxygenated complex. We explain this observation by the fact that the phenate in this particular spatial arrangement is facing the tripod and hence cannot approach the superoxo complex sufficiently to interact with it. In summary, this series of tren-capped iron(II) porphyrins represents the first example of a synthetic dioxygen carrier for which the very high affinity for dioxygen can be moderated by associating a low-pK_a phenol group with the cap. Concomitantly, as the tripod does not induce any steric hindrance close enough to the linear bound CO, no significant discrimination for the latter is observed, thereby confirming the crucial role of the steric factors for CO discrimination.

Acknowledgment. The authors thank the CNRS for financial support as well as the MENRT. C.R. is indebted to Région Bretagne for his grant. B.B. particularly acknowledges Région Bretagne for his significant financial support. D.R. thanks the MENRT for his Ph.D. grant.

Supporting Information Available: Spectroscopic data, including 1D, 2D NMR, electrospray HR-MS spectra, as well as detailed data for the $P_{1/2}$ measurements of the various new compounds and X-ray data for the crystal structure deposited at the Cambridge Crystallographic Data Center and allocated deposition number CCDC 273334. This material is available free of charge via the Internet at http://pubs.acs.org.

IC0514703